

Study on design of a noise covariance in pose estimation using 9-axis motion sensor

Hayato Sato, Kentaro Goto, Satoru Kizawa, and Ayuko Saito

Department of Mechanical Science and Engineering, Graduate School of Engineering, Kogakuin University,
Tokyo, Japan
E-mail: s519025@ns.kogakuin.ac.jp

Abstract

This paper presents an extended Kalman filter for pose estimation using noise covariance matrices based on sensor output. We designed three algorithms to accurately estimate the knee joint angle during walking. We verified the effectiveness of the algorithm by comparing them.

A Kalman filter has been mainly used in sensor fusion techniques for pose estimation. The Kalman filter is a sequential estimation and has the advantage that the calculation load is small. However, the estimation accuracy of pose estimation using the Kalman filter is greatly affected by the design of process and observation noise covariance. Therefore, in this study, we verified the accuracy of knee joint angle estimation during walking by using the process and observation noise covariance matrices of the extended Kalman filter based on the sensor output proposed in the previous study. The three types of algorithm were designed in this study. The first algorithm was designed which in only a process noise covariance matrix was based on the sensor output. The second algorithm was designed in which only an observation noise covariance matrix was based on the sensor output. The third algorithm was designed in which two noise covariance matrices were based on the sensor output. The effect of noise covariance matrices on estimation accuracy was considered by comparing the estimation results obtained from those algorithms.

The posture of the nine-axis motion sensor is represented by the roll angle (φ) around the X-axis, the pitch angle (θ) around the Y-axis, the yaw angle (ψ) around the Z-axis. The reference coordinate system is a right-handed system with a vertical Z-axis. The counterclockwise was rotation defined as positive. Euler definition and the reference coordinate system are represented in Fig.1. The nine-axis motion sensor is attached to the subject thing and lower leg. The local coordinate system of the sensor is converted system for the left knee angle estimation. ^[1]

The initial angles of roll and pitch can't be obtained from the output of the gyro sensor. The initial roll and pitch are expressed by equations (1) and (2) using the gravitational acceleration obtained from the acceleration sensor at rest.

$$\Phi_A = \tan^{-1} \frac{A_y}{A_z} \quad (-\pi < \varphi_A < \pi) \quad (1)$$

$$\theta_A = \tan^{-1} \frac{-A_x}{\sqrt{A_y^2 + A_z^2}} \quad (2)$$

where A_x , A_y and A_z are the accelerometer outputs.

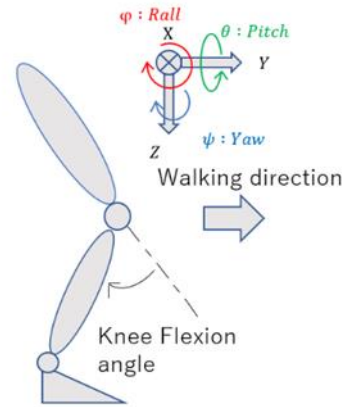


Fig.1. Reference coordinate system and the definition of knee joint angle

The initial Yaw is expressed by equation (3) after correcting the magnetic field disturbance and tilt error.

$$\Psi_m = \tan^{-1} \frac{c_{m_y}}{c_{m_x}} \quad (3)$$

The differential Euler angles are calculated by applying the gyro sensor output in equation (4).

$$\begin{bmatrix} \dot{\psi}_t \\ \dot{\theta}_t \\ \dot{\varphi}_t \end{bmatrix} = \begin{bmatrix} 0 & \sin\varphi_t \sec\theta_t & \cos\varphi_t \sec\theta_t \\ 0 & \cos\varphi_t & -\sin\varphi_t \\ 1 & \sin\varphi_t \tan\theta_t & \cos\varphi_t \tan\theta_t \end{bmatrix} \begin{bmatrix} \omega_t \\ \omega_t \\ \omega_t \end{bmatrix} \quad (4)$$

where $\dot{\varphi}_t$, $\dot{\theta}_t$, $\dot{\psi}_t$ are the differential Euler angles. Φ_t and θ_t are the roll and pitch angle at time t. ω_x , ω_y and ω_z the outputs the gyro sensor. Euler angles are obtained by applying equation (4) to equation (5).

$$\begin{bmatrix} \Psi_{t+1} \\ \theta_{t+1} \\ \varphi_{t+1} \end{bmatrix} = \int \begin{bmatrix} \dot{\psi}_t \\ \dot{\theta}_t \\ \dot{\varphi}_t \end{bmatrix} dt + \begin{bmatrix} \psi_t \\ \theta_t \\ \varphi_t \end{bmatrix} \quad (5)$$

where φ_{t+1} , θ_{t+1} , and ψ_{t+1} are the Euler angle.

The roll, pitch, and yaw angles of each sensor placed on the lower limb are estimated by the sensor fusion using the extended Kalman filter. The nonlinear state equation and nonlinear observation equation are shown in equations (6) and (7), respectively.

$$X_{t+1} = F(x_t) + w_t \quad (6)$$

$$x_t = \begin{bmatrix} \psi_{i,t} \\ \theta_{i,t} \\ \phi_{i,t} \end{bmatrix}, F(x_t) = \begin{bmatrix} \psi_{i,t} + \sin\phi_{i,t}\sec\theta_{i,t}\omega_{y_{i,t}} \cdot T_s + \cos\phi_{i,t}\sec\theta_{i,t}\omega_{z_{i,t}} \cdot T_s \\ \theta_{i,t} + \cos\phi_{i,t}\omega_{y_{i,t}} \cdot T_s - \sin\phi_{i,t}\omega_{z_{i,t}} \cdot T_s \\ \phi_{i,t} + \omega_{x_{i,t}} \cdot T_s + \sin\phi_{i,t}\tan\theta_{i,t}\omega_{y_{i,t}} \cdot T_s + \cos\phi_{i,t}\tan\theta_{i,t}\omega_{z_{i,t}} \cdot T_s \end{bmatrix}$$

$$y_t = H(x_t) + v_t \quad (7)$$

$$y_t = \begin{bmatrix} \psi_{m_{i,t}} \\ A_{x,s_i} \\ A_{y,s_i} \\ A_{z,s_i} \end{bmatrix}, H(x_t) = \begin{bmatrix} \psi_{i,t} \\ ({}^0R_i)^T \begin{bmatrix} 0 \\ 0 \\ g \end{bmatrix} \end{bmatrix}$$

In those equations, $\phi_{i,t}$, $\theta_{i,t}$, and $\psi_{i,t}$ respectively denote Euler angles of the sensor placed on each lower limb segment, as estimated using the extended Kalman filter. T_s is sampling time. In addition, $\omega_{x,t}$, $\omega_{y,t}$, and $\omega_{z,t}$ respectively denote the gyroscope outputs for the X, Y, and Z axes. Also, A_{S_x} , A_{S_y} , and A_{S_z} respectively express the accelerometer output for the X, Y, and Z axes. 0R_i is the rotation matrix from the reference coordinate system to the sensor i coordinate system, g is the gravitational acceleration, and w_t and v_t are the white noise. [2]

The partial derivatives of $F(x_t)$ and $H(x_t)$ are shown below:

$$f(x_t) = \frac{\partial F(x_t)}{\partial(x_t)} \quad (8)$$

$$h(x_t) = \frac{\partial H(x_t)}{\partial(x_t)} \quad (9)$$

Then, the prediction step [Eqs. (10) and (11)] and the filtering step [Eqs. (12)-(14)] are calculated using the nonlinear discrete-time system represented by Eqs. (8) and (9):

$$x_{\bar{t}+1} = F(x_t) \quad (10)$$

$$P_{\bar{t}+1} = f_t P_t f_t^T + Q \quad (11)$$

$$K_{t+1} = P_{\bar{t}+1} h_{t+1}^T (h_{t+1} P_{\bar{t}+1} h_{t+1}^T + R)^{-1} \quad (12)$$

$$x_{t+1} = x_{\bar{t}+1} + K_{t+1} (y_{t+1} - H(x_{\bar{t}+1})) \quad (13)$$

$$P_{t+1} = (I - K_{t+1} h_{t+1}) P_{\bar{t}+1} \quad (14)$$

Where P is the error covariance matrix, K is the Kalman gain, Q is the covariance matrix of the process noise w_t in the nonlinear state equation, and R is the covariance matrix of the observation noise v_t in the nonlinear observation equations. $x_{\bar{t}+1}$, $P_{\bar{t}+1}$ are the state variables and error covariance matrix at time $t+1$ estimated using the information up time to t . x_{t+1} , P_{t+1} are the state variables and error covariance matrix at time $t+1$ estimated using the information up to time $t+1$. [3]

The process and observation noise covariance matrices in the extended Kalman filter were

determined based on the state-space model dynamics and the sensor noise. The postural change appears in the gyroscope output because the rotational motion of the joints produces human movement. Consequently, the process noise covariance matrix was determined based on the gyroscope output as presented below:

$$Q_t = \begin{bmatrix} \Omega_{\omega,t} & 0 & 0 \\ 0 & \Omega_{\omega,t} & 0 \\ 0 & 0 & \Omega_{\omega,t} \end{bmatrix} \quad (15)$$

$$\Omega_{\omega,t} = a \sqrt{\omega_{x,t}^2 + \omega_{y,t}^2 + \omega_{z,t}^2}$$

$\omega_{x,t}$, $\omega_{y,t}$ and $\omega_{z,t}$ are gyro-sensor outputs for each axis, and a , b are the adjustment parameters. In this study, we set $a = 1$ and $b = 0$.

In the observation equations, the yaw angle calculated using the geomagnetic sensor output and the acceleration sensor output are used as observation values, so the covariance matrix of the process noise is adjusted based on the time series data of the geomagnetic sensor output and the acceleration sensor output. The constructed covariance matrix of the observation noise is shown in equation (16).

$$R_t = \begin{bmatrix} \Omega_{m,t} & 0 & 0 & 0 \\ 0 & \Omega_{a,t} & 0 & 0 \\ 0 & 0 & \Omega_{a,t} & 0 \\ 0 & 0 & 0 & \Omega_{a,t} \end{bmatrix} \quad (16)$$

$$\Omega_{m,t} = c \left(\sqrt{m_{x,t}^2 + m_{y,t}^2 + m_{z,t}^2} - \bar{m} \right) + d$$

$$\Omega_{a,t} = e \left(\sqrt{a_{x,t}^2 + a_{y,t}^2 + (a_{z,t} - g)^2} \right) + f$$

where $m_{x,t}$, $m_{y,t}$ and $m_{z,t}$ are the magnetometer outputs in each axis after tilt correction, \bar{m} is the average of the sum of the magnetometer outputs over the entire measurement time, $a_{x,t}$, $a_{y,t}$ and $a_{z,t}$ are the accelerometer outputs in each axis, and c , d , e and f are parameters for adjustment. We set $c = 0.1$, $d = 0$, $e = 0.00001$ and $f = 100$.

The knee joint angle is calculated by Eq. (17) as shown below:

$${}^{i-1}R_i = ({}^0R_{i-1})^T \cdot ({}^0R_i) \quad (17)$$

$${}^0R_i = \begin{bmatrix} \cos {}^i\psi & -\sin {}^i\psi & 0 \\ \sin {}^i\psi & \cos {}^i\psi & 0 \\ 0 & 0 & 1 \end{bmatrix} \begin{bmatrix} \cos {}^i\theta & 0 & \sin {}^i\theta \\ 0 & 1 & 0 \\ -\sin {}^i\theta & 0 & \cos {}^i\theta \end{bmatrix}$$

Sensor i and sensor $i-1$ indicate sensor attached to the thigh and lower leg, respectively.

A nine-axis motion sensor and an optical motion capture system were used during the experiment. A healthy male (height 1.76m, weight 58kg) participated in the experiment. The nine-axis motion sensor was attached to the left thigh and left lower leg. The sensor positions and the reference coordinate system are shown in Fig.2. The participant was instructed to walk using a natural stride in time with a metronome (70 bpm). The sampling frequency of both the nine-axis motion sensor and the three-dimensional motion analyzer was 100Hz.

Figure 3 shows the estimated left knee joint angles (flexion-extension) using the extended Kalman filter and the results obtained from the three-dimensional motion measurement analysis device. The horizontal axis is 100% for one gait cycle, and one gait cycle including one stance phase and one walking phase as 100%. Black solid curves represent results obtained from the optical 3D motion analysis system. Red solid curves represent results obtained from the extended Kalman filter using the noise covariance matrices based on sensor output, hereinafter designated as Oo and Op. Green solid curves represent results obtained from Oo and Op, which used gyroscope output for the process noise covariance matrix and which used a constant value for the observation noise covariance matrix, hereinafter designated as Op. Blue solid curves represent results obtained from Oo and Op, which used the constant value for the process noise covariance matrix and which used accelerometer and magnetometer output for the observation noise covariance matrix, hereinafter designated as Oo. The constant noise covariance matrix was adjusted to match the results of the three-dimensional motion analyzer, with $\Omega_\omega = 0.0005$ for the process noise covariance matrix and $\Omega_m = \Omega_a = 1500$ for the observation noise covariance matrix.

Fig. 3 shows that the proposed method Oo and Op is generally consistent with the result of the optical 3D motion analysis system. The proposed method was evaluated by using the root mean square error (RMSE) against the results of the optical 3D motion analysis system. The root mean square error is represented in Eq. (18).

$$RMSE = \sqrt{\frac{1}{n} \sum_{k=1}^n (f_i - y_i)^2} \quad (18)$$

The results of the RSME were Oo = 6.49 [degree], Op = 7.32[degree], and Oo and Op = 6.33[degree].

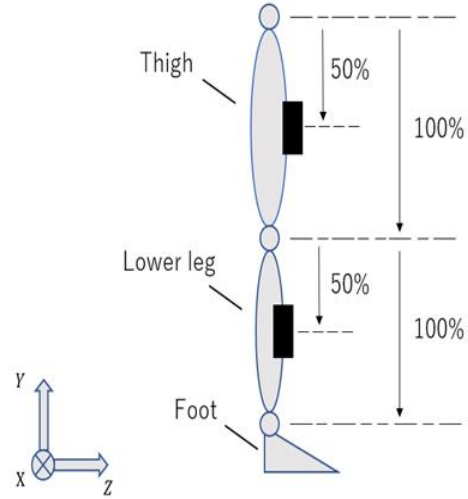


Fig.2. Sensor position and coordinate system

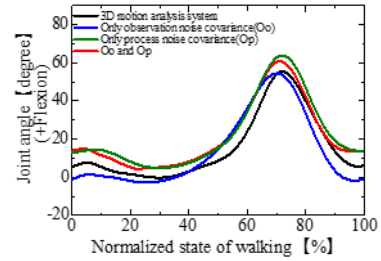


Fig.3. Knee joint angle during walking

As a result, we determined that Oo and Op are the suitable method for the pose estimation during walking.

In this study, we confirmed that the knee joint angle during walking can be estimated more accurately by adjusting the two noise covariance matrices based on the sensor output. However, the algorithm designed with the process noise covariance based on the sensor output and the observation noise covariance as a constant had lower estimation accuracy. In future work, we will build algorithms to minimize the environmental impact.

References:

- [1] Saito, A., Kizawa, S., Kobayashi, Y. and Miyawaki, K., Pose estimation by extended Kalman filter using noise covariance matrices based on sensor output, ROBOMECH Journal, Vol.7, No. 36 (2020), DOI: 10.1186/s40648-020-00185-y.
- [2] Hirose K, Doki H, Koda S, Nagasaku K (2011) Studies of the dynamic analysis and motion measurement of skiing turn using extended Kalman filter. Trans Jpn Soc Mech Eng, Series C 77(774):470–480 ((in Japanese))
- [3] Rigatos, G. G., Extended Kalman and Particle Filtering for sensor fusion in motion control of mobile robots, Mathematics and Computers in Simulation, Vol.81, No. 3 (2010), pp.590–607.